

Analyzing Object Detection Quality Under Probabilistic Coverage in Sensor Networks^{*}

Shansi Ren, Qun Li, Haining Wang, Xin Chen, and Xiaodong Zhang

College of William and Mary
Williamsburg, VA 23187, USA
{sren, liqun, hnw, xinchen, zhang}@cs.wm.edu

Abstract. Object detection quality and network lifetime are two conflicting aspects of a sensor network, but both are critical to many sensor applications such as military surveillance. Probabilistic coverage is an appropriate approach to balancing the conflicting design requirements of monitoring applications. Under probabilistic coverage, we present an analytical model to analyze object detection quality with respect to different network conditions and sensor scheduling schemes. Our analytical model facilitates performance evaluation of a sensing schedule, network deployment, and sensing scheduling protocol design. Applying the model to real sensor networks, we design a set of sensing scheduling protocols to achieve targeted object detection quality while minimizing power consumption. The correctness of our model and the effectiveness of the proposed protocols are validated through extensive simulation experiments.

1 Introduction

Sensor networks are used for a range of object detection and tracking applications, such as vehicle detection in military surveillance and wild animal habitat monitoring [9]. These applications, by their nature, enforce certain detection quality and lifetime requirements. The first requirement determines how fast a sensor network should detect the intrusion of a moving vehicle, or how often the data about a wild animal should be sampled and collected. The second requirement specifies the working duration a sensor network should sustain. These two requirements, however, are two conflicting optimization goals due to the stringent energy constraints of sensor nodes.

Full sensing coverage is mandatory for sensor monitoring applications that require either immediate response to detected events or information of all points in the sensing field. Full sensing coverage, however, is too restricted and expensive to support long-time monitoring applications. More often those applications do not need zero response time or information at all points of a sensing field. They may be willing to sacrifice some event detection delay or sensing fidelity

^{*} This work is supported in part by the U.S. National Science Foundation under grants CNS-0098055, CCF-0129883, and CNS-0405909.

to increase the network lifetime. Full sensing coverage gives little leverage to tune object detection quality and battery power consumption. A relaxed sensing coverage—probabilistic coverage where any point in a sensing field is sensed with a certain probability at any time—is a more appropriate approach to balancing object detection quality and battery power consumption.

Probabilistic coverage scheme allows sensor nodes to periodically wake up and go back to sleep. A node in sleep mode cannot sense events; its sensing capability is resumed after it wakes up. Therefore, the sensor network provides only a fraction of the maximal coverage of all the sensors. Battery power, however, is conserved for the nodes in sleep mode. How much time and how frequently a sensor node should stay in active mode determine detection quality and power saving. Our study aims to characterize the interplay among the sensor scheduling, detection quality and power saving.

In this paper, under probabilistic coverage, we present a mathematical model to analyze the object detection quality with respect to various network conditions such as the node density and the object moving speed, and sensor scheduling schemes including random sensing schedules and synchronized sensing schedules. Note that the full coverage can be incorporated into our model since it is just a special case of the probabilistic coverage. We define two metrics to assess the object detection quality: the sensor detection probability (DP), and the stealth distance (SD) that an object can stealthily pass. Applying the model to real sensor networks, we further design distributed random and localized algorithms to achieve targeted object detection quality while minimizing the power consumption. We validate the correctness of our model and the effectiveness of sensing scheduling protocols through extensive simulation experiments.

The contributions of our analytical model are threefold. First, this analytical model gives solid and thorough understanding about various protocols and provides insights into the pros and cons of each protocol. Even if some protocols are not amenable to easy analysis, we can approximate them and incorporate many of them into the model.

Second, the analytical model helps to plan a sensor network with certain object detection quality requirements and power budget. The model is flexible enough to capture the interaction among the system parameters (e.g., sensor density, sensing range, object moving speed, etc.), object detection quality requirements, and network energy constraint. Thus, it can provide accurate guidelines for optimal sensor network deployment, and can also derive the necessary speed of an object wanting to evade sensor detection.

Third, in sensing scheduling protocol design, aside from determining the parameters for sensing scheduling protocols, the analytical model can direct new sensing scheduling protocol design.

The remainder of this paper is organized as follows. Section 2 sketches related work. Section 3 presents the system metrics and parameters. Section 4 details the analytical models. We design a set of sensing protocols in Section 5. Section 6 studies energy consumption and system working time properties of different schedules and protocols. Section 7 shows analytical results and their simulation

validations. In Section 8 we apply our model to two formerly proposed protocols in the literature. Finally, we conclude our work in Section 9.

2 Related Work

Detecting and tracking a moving object in sensor networks has been extensively studied from different perspectives: maintaining high tracking precision [2, 5, 11], utilizing node collaborations [8, 15], and reducing energy consumption [10]. A large number of sensing coverage maintenance protocols, aiming to conserve energy under various conditions, have been proposed [1, 6, 12, 13]. The closest previous work to ours is [4], which is the first we believe to consider the trade-off between power conservation and quality of surveillance in target detection and tracking by using non-full coverage. [7] is an interesting work that gives the bound and asymptotic results on detectability. In [3], Cao *et al.* presented an optimized framework for rare event detection that compromises between event detection delay and lifetime while maintaining point coverage.

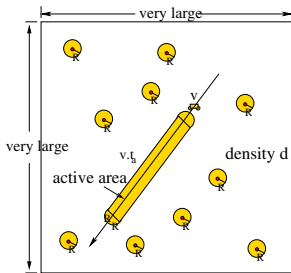
3 Object Detection Under Probabilistic Coverage

In order to evaluate the object detection quality of a sensor network, we define two metrics detailed as follows:

- *Detection Probability (DP)*. The detection probability is defined as the probability that an object is detected in a certain observation time.
- *Stealth Distance (SD)*. The stealth distance is defined as the average distance an object travels before it is detected for the first time.

Taking energy constraints into account, we further define other two metrics.

- *Lifetime (LT)*. The system lifetime is the elapsed working time from system startup to the time when the object detection quality requirement cannot be met for the first time when live nodes continue sensing with their current periods.



| parameter | definition |
|-----------|---------------------------------|
| d | density of sensors |
| R | sensing radius of a sensor |
| v | object moving speed |
| P | sensing period of sensors |
| f | active ratio of sensors in P |
| H | active duration $H = f \cdot P$ |
| t_a | observation duration |

Fig. 1. An object detection and tracking scenario

Fig. 2. System modeling parameters

- *Maximum Working Time.* The maximum working time is the longest possible working time of the system that satisfies the object detection quality requirement. When some nodes deplete their power, the remaining nodes can adjust their schedules to sustain the object detection quality.

Figure 1 shows a typical scenario of the object detection in a sensor network. A number of sensors with density d are randomly and independently distributed in a sensing field; the sensing radii of sensors have the same value R ; the sensors have the same sensing period P and the same active ratio f . There is a small moving object crossing over the field with a constant speed v along a specified direction. Note that the object size can be neglected considering the large dimensions of the sensing field. The observation duration is t_a . These system parameters of a sensor network are summarized in Figure 2.

Object detection applications may have different DP requirements and SD requirements. For given sensing scheduling schemes, we assess their object detection quality using DP and SD with respect to these system parameters. We study how each parameter affects the metrics, and how we can adjust them to reach the object detection quality goal while minimizing the energy consumption. Our simplified theoretical model can be easily applied to real applications because the real moving path can be approximated by a set of line segments, to each of which the analytical results can be directly applied.

4 Detection Quality Analysis Under Different Schedules

In this section, we present the theoretical analyses on how different scheduling schemes affect the object detection quality in terms of DP and SD. More specifically, we study random sensing schedules and synchronized sensing schedules. In a random sensing schedule, a node independently and randomly chooses the starting time of its active duration H in a sensing period P ; while in a synchronized sensing schedule, all nodes start their active duration H at the same time in every sensing period P . We compare these two schedules, and find that the random schedule performs better generally, while the synchronized schedule has a better worst case object non-detecting traveling distance in multiple experiments.

4.1 Random Sensing Schedule Analysis

A random sensing schedule is a simple but usually efficient schedule due to its distributed nature. It can serve as a baseline for analysis of and comparison to other schedules.

We first analyze the DP and the SD when sensors have the same sensing period P . Then we study the DP for a special case of fast objects. We introduce this special case analysis because it yields more simplified numerical results, which eases choosing appropriate network parameters to achieve required object detection quality while minimizing energy consumption. Finally we study how

nodes can sense with different periods to achieve the same DP as those having the same period for fast objects.

Detection Probability. We study random sensing schedules in which all the nodes have the same sensing period P and the same active duration H .

Consider a moving object moves from left to right on x -axis. Suppose it starts at the point $-\frac{vt_a}{2}$, travels a distance of vt_a , and arrives at the point $\frac{vt_a}{2}$ during the observation duration t_a . Define the *active area* AA of this object as the oblong area in Figure 3, including the rectangle area with length vt_a and width of $2R$, and the two half disks with radius R attached to the rectangle. We can see that $AA = vt_a \cdot 2R + \pi R^2$.

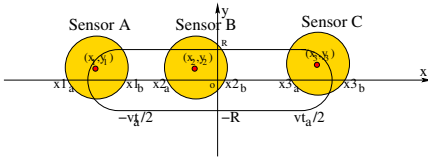


Fig. 3. Three sensors are located in the active area of a moving object

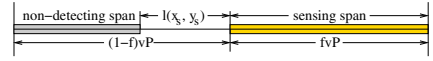


Fig. 4. The distance an object crosses in one sensing period

Proposition 1. Let $Pr(x_s, y_s)$ denote the detection probability of a sensor located at (x_s, y_s) in the active area within t_a , and $\tilde{P}r$ denote the probability that one single sensor can detect this object within t_a , then

$$\tilde{P}r = \frac{1}{AA} \int_{-R}^R dy_s \int_{-\frac{vt_a}{2}-R}^{\frac{vt_a}{2}+R} Pr(x_s, y_s) dx_s. \quad (1)$$

Proof: For a specific sensor located at position (x_s, y_s) to detect this object, two conditions must be satisfied: the sensor must be in the active area; the sensor must be active when the object crosses its sensing range. The detection probability of this sensor depends on the length of the segment that the object moving path intersects its sensing range. As shown in Figure 3, when the sensor is located at different parts in the active area, the intersecting length $l(x_s, y_s)$ has different representations. Then we have $l(x_s, y_s) = \min(\frac{vt_a}{2}, x_b) - \max(-\frac{vt_a}{2}, x_a)$, where $x_a = x_s - \sqrt{R^2 - y_s^2}$ and $x_b = x_s + \sqrt{R^2 - y_s^2}$ are the x coordinates of two intersecting points.

According to Figure 4, the detection probability of this sensor is $Pr(x_s, y_s) = f + \frac{t}{P}$ when $l(x_s, y_s) < (1-f)vP$ or $Pr(x_s, y_s) = 1$ when $l(x_s, y_s) \geq (1-f)vP$, where $t = \frac{l(x_s, y_s)}{v}$. Notice that $l(x_s, y_s) = 0$ and $Pr(x_s, y_s) = 0$ when (x_s, y_s) is outside the active area. Then, $\tilde{P}r$ can be obtained by computing the expectation of $Pr(x_s, y_s)$ over the active area as in (1). \square

For the case of multiple sensors, since the nodes are randomly deployed, the number of sensors in the active area follows a Poisson distribution with an expected value of $\lambda = d \cdot AA$.

Theorem 1. *The detection probability under the random sensing schedule is*

$$DP = 1 - e^{-\lambda \tilde{P}r}. \tag{2}$$

Proof: The probability that there are k sensors in the active area is $Pr(k) = \frac{e^{-\lambda} \cdot \lambda^k}{k!}, k = 0, 1, \dots, \infty$, while the probability that there exists k sensors in the active area and at least one of them can detect this object is $Pr(dt \wedge k) = \frac{e^{-\lambda} \lambda^k}{k!} [1 - (1 - \tilde{P}r)^k]$. Particularly, when $k = 0$, we have $Pr(0) = \frac{e^{-\lambda} \cdot \lambda^0}{0!} = e^{-\lambda}$. Because $\sum_{k=0}^{\infty} \frac{e^{-\lambda} \cdot \lambda^k}{k!} = 1$, we have $\sum_{k=1}^{\infty} \frac{e^{-\lambda} \cdot \lambda^k}{k!} = 1 - e^{-\lambda}$. Also $Pr(0) = \frac{e^{-\lambda} \lambda^0 (1 - \tilde{P}r)^0}{0!} = e^{-\lambda}$, and $\sum_{k=0}^{\infty} \frac{e^{-\lambda} \lambda^k \cdot (1 - \tilde{P}r)^k}{k!} = e^{-\lambda \tilde{P}r}$. Then, we get $DP = \sum_{k=1}^{\infty} Pr(dt \wedge k) = \sum_{k=1}^{\infty} \frac{e^{-\lambda} \cdot \lambda^k}{k!} [1 - (1 - \tilde{P}r)^k] = (1 - e^{-\lambda}) - (e^{-\lambda \tilde{P}r} - e^{-\lambda}) = 1 - e^{-\lambda \tilde{P}r}$. \square

Stealth Distance. The stealth distance is an important metric to characterize the object detection quality. Here we derive the stealth distance for the random sensing schedule.

Theorem 2. *The stealth distance under the random sensing scheme is*

$$SD = \int_0^{\infty} v e^{-\lambda \tilde{P}r} dt_a. \tag{3}$$

Proof: Denote $cdf(x)$ and $pdf(x)$ as the cumulative distribution function and the probability density function of a numerical random variable x . We know $cdf'(x) = pdf(x)$. Also define $(1 - cdf)(x) = 1 - cdf(x)$.

The DP in (2) is a cdf function that can be written in the form of $Pr(t \leq t_a)$, where t is the point that the object is detected for the first time, and t_a can be viewed as a variable. Thus, $(1 - cdf)(t_a) = Pr(t > t_a) = e^{-\lambda \tilde{P}r}$. Because $\lim_{t_a \rightarrow \infty} cdf(t_a) = 1$, and $\lim_{t_a \rightarrow \infty} (1 - cdf)(t_a) = 0$, and they approach their limits exponentially when t_a approaches ∞ linearly, we have the expected detecting time $E(t_a) = \int_0^{\infty} pdf(t_a) \cdot t_a dt_a = \int_0^{\infty} (1 - cdf)(t_a) dt_a$. Therefore, $E(t_a) = \int_0^{\infty} e^{-\lambda \tilde{P}r} dt_a$. Thus, $SD = vE(t_a) = \int_0^{\infty} v e^{-\lambda \tilde{P}r} dt_a$. \square

Detection Probability For Fast Objects. For fast objects, we can have more simplified numerical results for the detection probability, as described in the following corollary.

Corollary 1. *We consider a special case, in which an object moves with a high speed v such that $vt_a > 2R$ and $(1 - f)vP > 2R$. Then, the probability of a single sensor detecting this fast object is*

$$\tilde{P}r = f + \frac{\pi R^2 t_a}{(vt_a \cdot 2R + \pi R^2)P}. \tag{4}$$

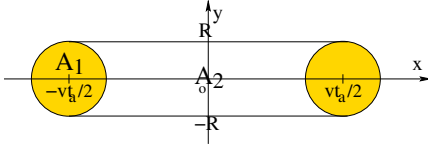


Fig. 5. The active area for detection probability calculation

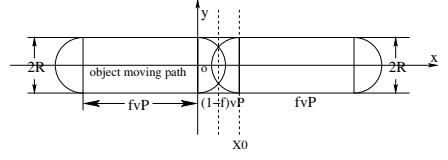


Fig. 6. The active area in the synchronized schedule when R is large

Proof: For this object, we get $\tilde{P}r = f + \frac{1}{AvP} \int_{-\frac{vt_a}{2}-R}^{\frac{vt_a}{2}+R} dx_s \int_{-R}^R l(x_s, y_s) dy_s$ if we simplify (1).

Consider a sensor s located at (x_s, y_s) . Denote $\xi_1 = \iint_{A_1} l(x_s, y_s) dx_s dy_s$, and $\xi_2 = \iint_{A_2} l(x_s, y_s) dx_s dy_s$, where A_1 is the circle on the left and A_2 is the unfilled area in the middle as shown in Figure 5. Due to the symmetry of the integrating area, we have $\int_{-\frac{vt_a}{2}-R}^{\frac{vt_a}{2}+R} dx_s \int_{-R}^R l(x_s, y_s) dy_s = 2\xi_1 + \xi_2$.

Let x_a and x_b ($x_b > x_a$) be the x coordinates of the two intersecting points between the object path and the sensing circle of node s . Notice that $l(x_s, y_s) = \max(x_b, -\frac{vt_a}{2}) - \max(x_a, -\frac{vt_a}{2})$ when $(x_s, y_s) \in A_1$. Now we compute $l(x_s, y_s)$ under following conditions:

- $x_b > x_a > -\frac{vt_a}{2}$. We have $x_s > \sqrt{R^2 - y_s^2} - \frac{vt_a}{2}$ and $l(x_s, y_s) = x_b - x_a = 2\sqrt{R^2 - y_s^2}$.
- $x_b > -\frac{vt_a}{2}$ and $x_a < -\frac{vt_a}{2}$. We have $-\frac{vt_a}{2} - \sqrt{R^2 - y_s^2} < x_s < -\frac{vt_a}{2} + \sqrt{R^2 - y_s^2}$ and $l(x_s, y_s) = x_b + \frac{vt_a}{2} = x_s + \frac{vt_a}{2} + \sqrt{R^2 - y_s^2}$.
- $x_b < -\frac{vt_a}{2}$ and $x_a < -\frac{vt_a}{2}$. We have $l(x_s, y_s) = 0$.
- $x_b < -\frac{vt_a}{2}$ and $x_a > -\frac{vt_a}{2}$. Because $x_b > x_a$, this case is impossible.

We can get $\xi_1 = \int_{-R}^R dy_s \int_{-\sqrt{R^2 - y_s^2} - \frac{vt_a}{2}}^{\sqrt{R^2 - y_s^2} - \frac{vt_a}{2}} (x_s + \frac{vt_a}{2} + \sqrt{R^2 - y_s^2}) dx_s = \frac{8R^3}{3}$,

and $\xi_2 = \int_{-R}^R dy_s \int_{\sqrt{R^2 - y_s^2} - \frac{vt_a}{2}}^{\sqrt{R^2 - y_s^2} + \frac{vt_a}{2}} 2\sqrt{R^2 - y_s^2} dx_s = \pi R^2 vt_a - \frac{16R^3}{3}$. Therefore,

$2\xi_1 + \xi_2 = \pi R^2 vt_a$. We can get $\tilde{P}r = f + \frac{1}{AvP} (2\xi_1 + \xi_2)$, which leads to (4). \square

Sequential Schedule and k -Set Schedule. As an extension of our previous results, here we show two equivalent scheduling schemes that can achieve the same detection quality as the random schedule with a constant sensing period P . We assume $2R < (1-f)vP$, which implies that $l(x_s, y_s)$ is always less than $(1-f)vP$, and H is a constant. Under these assumptions, according to (2), we know $\tilde{P}r$ can be written in the form of $\frac{a}{P}$, where a is a variable that is independent of P and λ . In the following analysis, we only vary P and λ while leaving all other system parameters unchanged.

Lemma 1. *Let A be a schedule with sensing period kP and λ , where k is a non-negative value. We randomly divide the nodes into k equal-sized sets, and nodes in*

each set are randomly distributed in the field. Consider a sequential schedule B , where nodes in i th set are active only in the duration of $[(i-1)P+nkP, iP+nkP)$ for $1 \leq i \leq k$, then the schedule A and the schedule B have identical detection probability, i.e., $DP_A = DP_B$.

Proof: In schedule B , all sets have identical detection probabilities. Consider the i th set S_i , the detection probability is $DP_B(S_i) = 1 - e^{-\frac{\lambda}{k}\hat{P}r} = 1 - e^{-\frac{\lambda\alpha}{k\hat{P}}}$, which is the same as that of schedule A . \square

Lemma 2. We randomly divide the nodes into k sets S_1, S_2, \dots, S_k . For any set S_i with density $x_i\lambda$, we associate a sensing period g_iP with it. Let $DP(S_i)$ denote the DP for the nodes in set S_i . If $\frac{x_1}{g_1} + \frac{x_2}{g_2} + \dots + \frac{x_k}{g_k} = 1$, then the detection probability DP of this k -set schedule is equal to that of the schedule with all nodes having the same period P .

Proof: We know that $DP(S_i) = 1 - e^{-x_i\lambda \cdot \frac{\alpha}{g_iP}}$. Let $\overline{DP(S_i)}$ be the probability that no node in S_i detects this object, so $\overline{DP(S_i)} = 1 - DP(S_i) = e^{-x_i\lambda \cdot \frac{\alpha}{g_iP}}$. Thus, we have $DP = 1 - \overline{DP(S_1)} \cdot \overline{DP(S_2)} \cdot \dots \cdot \overline{DP(S_k)} = 1 - e^{-\frac{\lambda\alpha}{P}(\frac{x_1}{g_1} + \frac{x_2}{g_2} + \dots + \frac{x_k}{g_k})} = 1 - e^{-\frac{\lambda\alpha}{P}}$. \square

4.2 Synchronized Sensing Schedule Analysis

A synchronized sensing schedule has the benefit that the worst case object non-detecting traveling distance is relatively small. Given that the field is fully covered by all active sensors, the worst case object non-detecting traveling distance is bounded by the maximum distance this object travels in one sensing period. Under synchronized sensing schedule, we first analyze the DP under the given system parameters. Based on the DP analysis, we then derive the SD. Note that all nodes have the same sensing periods here.

Detection Probability. Similar to the random sensing analysis, we study the active area under a synchronized sensing schedule to derive the detection probability.

Consider the traveling distance of a moving object in one sensing period P , we divide it into two parts: the first part is the distance the object travels in the duration $(1-f)P$ when all sensors are asleep; the second part is the distance the object travels when all sensors are active. In the first part, the object cannot be detected by any sensor; however, in the second part, the object can be detected when there are active sensors within a distance of R to it. Define the *active area* AA of a moving object as the set of points that are within a distance of R to the second part traveling segments of this object.

As shown in Figures 6, AA is the set of periodically repeated areas, except the last one when t_a is not multiple times of P . Each repeated area is either a rectangle plus two overlapped half circles (shown in Figure 6), or a rectangle plus two disjoint half circles. Denote $X_0 = (1-f)vP$ as shown in Figures 6. We assume that $t_a > P$.

Let $IA(P)$ be the total covering area of two half disks in one intermediate sensing period P . We consider whether there is overlapping in $IA(P)$. When $R \geq \frac{X_0}{2}$, intersecting points of two half disks are $(\frac{X_0}{2}, -\sqrt{R^2 - \frac{X_0^2}{4}})$ and $(\frac{X_0}{2}, \sqrt{R^2 - \frac{X_0^2}{4}})$. Then $IA(P) = 4 \int_0^{\frac{X_0}{2}} \sqrt{R^2 - x^2} dx = X_0 \sqrt{R^2 - \frac{X_0^2}{4}} + 2R^2 \arcsin \frac{X_0}{2R}$. When $R < \frac{X_0}{2}$, $IA(P) = \pi R^2$. Therefore, the active area in one intermediate sensing period P is $AA(P) = IA(P) + 2RvfP$.

To calculate the detection probability, we have the following theorem.

Theorem 3. *During the observation duration t_a , the active area is $AA(t_a) = \pi R^2 - IA(P) + \frac{t_a IA(P)}{P} + 2Rvft_a$. Let λ_s be the expected number of sensors in the active area, $\lambda_s = d \cdot AA(t_a)$. Then*

$$DP = 1 - e^{-\lambda_s} \quad (5)$$

Proof: The probability that no sensor in the active area is $e^{-\lambda_s}$. So, the detection probability that at least one sensor can detect this object under the synchronized sensing schedule is $DP = 1 - e^{-\lambda_s}$. \square

Stealth Distance. Based on the above DP result, we can immediately derive the stealth distance for the synchronized sensing schedule. We have the following theorem.

Theorem 4. *The stealth distance SD under synchronized sensing schedule is*

$$SD = \frac{vP}{d \cdot (IA(P) + 2RvfP)} e^{-d(\pi R^2 - IA(P))}. \quad (6)$$

Proof: Similar to the random sensing analysis, we can view t_a in DP as a variable. We know $(1 - cdf)(t_a) = 1 - DP = e^{-d(\pi R^2 + IA(P))} \cdot e^{-d(\frac{IA(P)}{P} + 2Rvf)t_a}$. Let $F'(t_a) = (1 - cdf)(t_a)$, then $F(t_a) = \frac{-Pe^{-d(\pi R^2 - IA(P))}}{d(IA(P) + 2RvfP)} e^{-d(\frac{IA(P)}{P} + 2Rvf)t_a} + C$, where C is constant.

Let $E(t_a)$ be expected detecting time, we have $E(t_a) = \int_0^\infty (1 - cdf)(t_a) dt_a$, then $E(t_a) = F(t_a)|_0^\infty = \frac{Pe^{-d(\pi R^2 - IA(P))}}{d(IA(P) + 2RvfP)}$. So $SD = vE(t_a) = \frac{vP}{d \cdot (IA(P) + 2RvfP)} \cdot e^{-d(\pi R^2 - IA(P))}$. \square

Now we study a special case of $f = 100\%$, which means nodes wake up the whole time and never sleep. We have $(1 - cdf)(t_a) = e^{-d\pi R^2 - 2dRvt_a}$, therefore

$$SD = \int_0^\infty v e^{-(d\pi R^2 + 2dRvt_a)} dt_a = \frac{e^{-d\pi R^2}}{2dR}. \quad (7)$$

5 Design of Power Efficient Sensing Protocols

In this section, we design three practical sensing protocols that ensure: (I) the object detection quality requirement is satisfied; (II) low sensing duty cycles

are utilized to save sensing energy; and (III) only moderate communication and computation overhead are incurred. The protocols are detailed as follows. Note that H is fixed in these protocols and there are n sensors in the network.

(I) *Global Random Schedule (GRS)*: The global density d is known to all sensors. According to Theorem 1, each node senses the field with the maximum sensing period P_{max} that satisfies the DP requirement.

(II) *Localized Asynchronous Schedule (LAS)*: This protocol is based on the fact that sensors in a dense region can have a larger P than those in a scarce region to reach the same object detection quality. After a node boots up, it broadcasts beaconing messages and infers the relative distance to its neighbors based on their signal strength. Then, it computes its local node density d_l by dividing the number of nodes in its communication range over the area of that range. According to Theorem 1, each node uses its local density d_l to compute the maximum period P_{max} that meets the object detection quality requirement as its sensing period. So, this algorithm achieves an object detection quality close to the targeted one.

(III) *Power-Aware Asynchronous Schedule (PAAS)*: This protocol takes the diversity of power capacity among sensor nodes into consideration. The whole set of nodes is divided into k sets S_1, S_2, \dots, S_k , such that all nodes in set S_i have approximately the same power capacity E_i , where $1 \leq i \leq n$. Based on Lemma 2, we can set $g_i = \frac{\sum_{i=1}^k x_i E_i}{E_i}$ to achieve the same object detection quality as GRS does with a constant sensing period P for each node. If each set has one and only one node, given the sum of the power capacities $E = \sum_{i=1}^n E_i$, we can schedule a node that has a power capacity E_i with a sensing period $\frac{E}{nE_i}P$ to achieve the same object detection quality as GRS protocol does.

6 Energy Consumption and Working Time Analysis

We assume in all schedules the active duration H lasts long enough so that we can ignore the wake-sleep transition energy cost. System lifetime is a critical factor that indicates the quality of the sensor network, since the energy resource is an extremely scarce resource in each node. Let T be the continuous working time of a single node, and all nodes have the same T . Under the random sensing schedule and the synchronized sensing schedule, if all nodes have the same P and the same f , then one node spends H energy in a period P . This node will last for $\frac{T}{H}$ periods, thus its working time is $\frac{T}{H} \cdot P = \frac{T}{f}$. Therefore, the system lifetime is $LT = \frac{T}{f}$. Particularly, when H is constant, $LT = \frac{T}{f} = \frac{TP}{H}$, this means that a small f or a large P can yield a long system lifetime.

Define the first failure time and the last failure time as the time when the first live node and the last live node in the system deplete their power. For a sensor network with n nodes, we denote T_i as the time when the i th node runs out of its power for $i = 1, 2, \dots, n$, and define T_f and T_l as the first failure time and the last failure time of the network. Note that H is fixed here.

In GRS, all nodes have the same sensing period P and the same active ratio f . Therefore, $T_i = \frac{E_i}{f}$ for $i = 1, 2, \dots, n$. So, $T_f(\text{GRS}) = \min(T_1, T_2, \dots, T_n) = \min(\frac{E_1}{f}, \frac{E_2}{f}, \dots, \frac{E_n}{f})$. In PAAS, because nodes have different sensing period, they have different active ratio as well. Let P and f be the fixed sensing period and the fixed active ratio in the GRS protocol, respectively. Denote f_i as the active ratio of the i th node, where $i = 1, 2, \dots, n$, then we have $f_i = \frac{H}{g_i P}$. On the other hand, because $g_i P = \frac{E}{n E_i} P$, we can get $f_i = \frac{n f E_i}{E}$. Note that in PAAS, all nodes have the same elapsed working time, i.e., $T_f = T_l = T_1 = T_2 = \dots = T_n$. Therefore, $T_f(\text{PAAS}) = \frac{E}{n f}$. Because $\frac{E}{n} \geq \min(E_1, E_2, \dots, E_n)$, we know $T_f(\text{GRS}) \leq T_f(\text{PAAS})$. In other words, PAAS has a larger first failure time than GRS.

The maximum working time is always longer than the lifetime in the previous definition, thus it can better characterize the energy consumption property of the network. Here we consider a *simple random sensing schedule*, in which all nodes have identical sensing periods at any moment, and only wake up once in one sensing period. We have the following theorem.

Theorem 5. *With the same DP requirement, the simple random sensing schedule and the PAAS have the same energy consumption rate, thus have the same maximum working time.*

Proof: We know $DP = 1 - e^{-\lambda c/P}$, where c is a constant if H and other detection parameters are fixed. The energy consumption per time unit that meets the required detection quality is fixed and is proportional to λ/P . This is because the number of participating sensors is proportional to λ , and the energy consumption of each sensor is proportional to $1/P$. Therefore, for any simple random sensing schedule with a given detection probability requirement, the energy consumption rate is $n f$, where n is the total number of nodes and f is the active ratio of each sensor node.

For the PAAS, even though each node sets its P according to its remaining power, the total power consumption of all nodes is still constant. Consider the i th node in all n nodes, where $1 \leq i \leq n$. Its energy consumption rate is $er_i = \frac{H}{P_i}$. Because $P_i = \frac{E}{n E_i}$ and H is constant, then $er_i = \frac{H}{P_i} = \frac{H}{\frac{E}{n E_i}} = \frac{n H E_i}{E P}$. The total energy consumption rate is $\sum_{i=1}^n er_i = \sum_{i=1}^n \frac{n H E_i}{E P} = \frac{n f E P}{E P} = n f$. Therefore, the PAAS has the same maximum working time as the simple random schedule, in which all nodes have fixed sensing periods. \square

7 Analysis Validation and Protocol Evaluation

In our simulation experiments, we generated a 500×500 grid field, and randomly placed $d \times 250,000$ sensors on it. Sensors use either random sensing schedule or synchronized sensing schedule. A small object moves along a straight line with a constant speed v . We run each simulation scenario for hundreds of times. Then, we use the ratio of detection times over the number of experiments to estimate DP, and use the average non-detecting distance to estimate SD.

7.1 Evaluation of Random and Synchronized Schedules

We plot both analytical curves and simulation results under different combinations of six parameters as shown in Figures 7, 8, and 9, respectively. Our observations are summarized as follows: (I) The simulation results match the analytical curves well, which validates the correctness of our derivations. (II) DP monotonically increases, and SD monotonically decreases with the increase of the parameters, as shown in Figure 10. (III) The random schedule outperforms the synchronized schedule on both DP and SD, which is shown in Figure 9. This is because the synchronized schedule causes more overlapping sensing areas than the random schedule. (IV) The non-detecting distance distributions have long tails: most non-detecting distances are short, while a few have large values. The worst case of non-detecting distance in the random schedule is longer than that of the synchronized schedule.

7.2 Evaluation of GRS, LAS, and PAAS Protocols

We use the DP to evaluate the effectiveness of the GRS, LAS, and PAAS protocols, and use the first failure time, the last failure time, and the system lifetime to compare their power consumption properties.

In our experiments to evaluate these three protocols, each sensor node’s energy follows a uniform distribution between $[0, E_{max}]$. We set system parameters as follows: $d = 0.2, R = 0.5, v = 5, t_a = 2, P = 1.1, H = 0.55, r = 3$, and

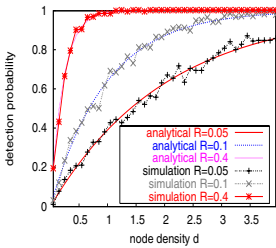


Fig. 7. DP under the random schedule. $v = 1, t_a = 5, P = 0.1, f = 0.5$

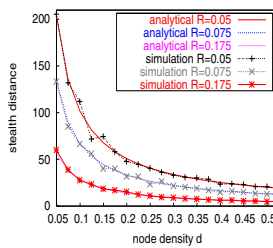


Fig. 8. SD under the random schedule, $v = 1, P = 0.1, f = 0.5$

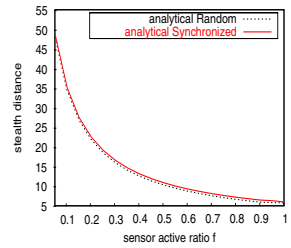


Fig. 9. SD under the two schedules. $d = 0.4, R = 0.2, v = 2, P = 2$

| metric | $d \uparrow$ | $R \uparrow$ | $v \uparrow$ | $t_a \uparrow$ | $P \uparrow$ | $f \uparrow$ |
|--------|--------------|--------------|--------------|----------------|--------------|--------------|
| DP | \uparrow | \uparrow | \uparrow | \uparrow | \uparrow | \downarrow |
| SD | \downarrow | \downarrow | \uparrow | | \downarrow | \uparrow |

Fig. 10. DP and SD change when system parameters increase

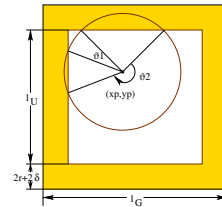


Fig. 11. Uncovered square of one grid in the Mesh protocol

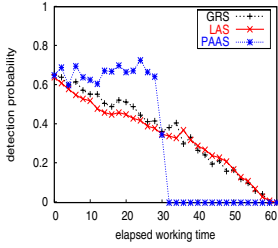


Fig. 12. DP comparison between GRS, LAS, and PAAS

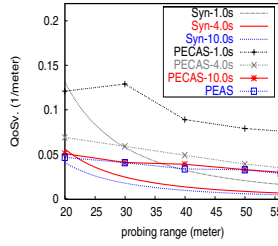


Fig. 13. QoS_v under the synchronized schedule compared to that in [4]

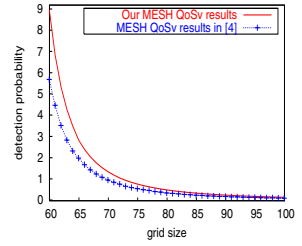


Fig. 14. QoS_v of the Mesh protocol compared to that in [4]

$E_{max} = 30$. Here r is the range to compute the local density in LAS. Given the requirement of $DP \geq 60\%$, Figure 12 illustrates the degradation of DP as nodes run out of power. Note that every data point in this figure is obtained by averaging hundreds of experiment results.

Based on the simulation results, we have the following observations: (I) GRS, LAS, and PAAS can achieve the same DP at the beginning when no sensor depletes its energy. (II) The first failure time and the last failure time of PAAS are the same; by contrast, GRS and LAS have smaller first failure time and larger last failure time. (III) PAAS has a longer system lifetime than those of GRS and LAS. (IV) The DP degradation curves of GRS and LAS in Figure 12 are exponential, instead of linear. This is because for a sensor whose energy is uniformly distributed in $[0, E_{max}]$, the DP at time t is $DP(t) = 1 - e^{-\lambda(t)\bar{P}r}$, where $\lambda(t) = \lambda_0 - qt$, q is the death rate, and λ_0 is the initial sensor density. Thus, $DP(t) = 1 - e^{\lambda_0\bar{P}r} \cdot e^{qt\bar{P}r}$.

8 Applying the Model to PECAS Protocol and Mesh Protocol

We further apply our analytical model to two sensing schedules in the literature, namely PECAS and Mesh. We show that by choosing appropriate parameters these schedules can be approximated by the random sensing schedule and the synchronized sensing schedule. In particular, we present the analytical QoS_v results on the PECAS protocol, while in [4] only simulation results are given.

8.1 Analysis of the PECAS Protocol

The PECAS protocol [4] is an enhanced variance of the Probing Environment and Adaptive Sleeping (PEAS) protocol [14]. In PECAS, each node remains active only for a limited duration. Here we extract the network parameters out of the PECAS experiments in [4]. Let the node density of the field be d , and the probing range of a node be r . In a circle area of πr^2 , the ex-

pected number of nodes is $d \cdot \pi r^2$. Because $d \cdot f = \frac{1}{\pi r^2}$, on average the active ratio of a node is $f = \frac{1}{d\pi r^2}$. The system parameters in [4] are as follows: $d = \frac{800}{400m \times 400m} = 0.005/m^2$, $R = 20m$, $v = 10m/s$, and r varies from $20m$ to $56m$. Since $f = \frac{1}{d\pi r^2}$, we know f changes from 0.159 (when $r = 20m$) to 0.0203 (when $r = 56m$). The working time duration in the three curves in [4] is 1.0sec, 4.0sec, and 10.0sec, respectively. This duration is H in the random schedule and the synchronized schedule. On the other hand, the QoS_v is the reciprocal of the SD, i.e., $QoS_v = 1/SD$.

With these parameter settings, we plot the corresponding QoS_v under the random and the synchronized sensing schedules as well as the PECAS curves in [4]. A larger probing range r or a larger working time duration results in a smaller QoS_v . We find that the random sensing schedule has a better QoS_v than PECAS for the reason that a small node density d incurs a small chance of nodes being close to each other. On the other hand, the synchronized sensing schedule has a similar QoS_v result to that of the PECAS protocol, as shown in Figure 13. In the PECAS, once a node goes into sleep, there are several nodes around it wake up. This is similar to the scenario where nodes all wake up simultaneously in the synchronized schedule.

8.2 Analysis of the Mesh Protocol

In the Mesh protocol [4], nodes at planned locations remain active and form a planned pattern of 2-D mesh by a set of horizontal and vertical solid lines. The distance between adjacent horizontal or vertical lines is L_G . Each uncovered area in this sensor deployment is a square with a side length of L_u , where $L_u = L_G - 2r - 2\delta$, as shown in Figure 11.

If the node density is high, for a randomly chosen point, its probability of not being covered by any active sensor is $Pr_{uc} = \frac{(\lfloor \frac{L}{L_G} \rfloor)^2 (L_G - 2r - 2\delta)^2}{L^2}$. As shown in Figure 11, for the point with coordinate (x_p, y_p) in the uncovered square, we draw a disk centered at it with a radius of vt_a . Denote $\xi = \frac{L_u}{2}$. Suppose there are $2m$ intersecting points between this disk and the four border lines, then the circle is divided into arcs by the intersecting points, interleavingly inside and outside the uncovered square. Let the angles of these arcs inside be $\theta_1(x_p, y_p), \dots, \theta_m(x_p, y_p)$. By definition, the average DP at the point (x_p, y_p) is $\frac{\sum_{i=1}^m \theta_i}{2\pi}$. We integrate the average DP of a point over the whole uncovered square to obtain the DP in t_a :

$$DP_{mesh} = \frac{(\lfloor \frac{L}{L_G} \rfloor)^2 \int_{-\xi}^{\xi} dx_p \int_{-\xi}^{\xi} (\frac{\sum_{i=1}^m \theta_i(x_p, y_p)}{2\pi}) dy_p}{L^2}.$$

We use the same parameter settings as that in [4], which are listed as follows: $l = 400m$, $R = 20m$, $v = 10m/s$, L_G varies from $60m$ to $100m$, $l_U = l_G - 10m$, and $2\delta = 10m$. The DP here is a *cdf* function of the variable t_a . We integrate the $(1 - cdf)$ function over the time span of $[0, \infty)$ to obtain the SD, then $QoS_{v_{mesh}} = \frac{1}{\int_0^{\infty} DP_{mesh} dt_a}$. The comparison between our results and the results in [4] is illustrated in Figure 14. The close match of the two curves validates the correctness of both analyses.

9 Conclusion

Balancing object detection quality and network lifetime is a challenging task in sensor networks. Under probabilistic coverage, we present an analytical model to fully investigate object detection quality with respect to various network conditions and sensing scheduling protocols. Based on the model, we design and analyze a number of sensing protocols. The correctness of our analytical model and the effectiveness of the proposed scheduling protocols are justified through extensive simulation experiments.

Acknowledgment

We thank the anonymous reviewers for their constructive comments and suggestions. We are also grateful to William L. Bynum for reading an early draft of this paper.

References

1. Z. Abrams, A. Goel, and S. Plotkin. Set K-Cover algorithms for energy efficient monitoring in wireless sensor networks. In *Proceedings of IPSN'04*.
2. J. Aslam, Z. Butler, F. Constantin, V. Crespi, G. Cybenko, and D. Rus. Tracking a moving object with a binary sensor network. In *Proceedings of ACM SenSys'03*.
3. Q. Cao, T. Abdelzaher, T. He, and J. Stankovic. Towards optimal sleep scheduling in sensor networks for rare-event detection. In *Proceedings of IPSN'05*.
4. C. Gui, and P. Mohapatra. Power conservation and quality of surveillance in target tracking sensor networks. In *Proceedings of ACM MobiCom'04*.
5. R. Gupta, and S. R. Das. Tracking moving targets in a smart sensor network. In *Proceedings of IEEE VTC Fall 2003 Symposium*.
6. C. Hsin, and M. Liu. Network coverage using low duty-cycled sensors: random & coordinated sleep algorithms. In *Proceedings of IPSN'04*.
7. B. Liu, and D. Towsley. A study on the coverage of large-scale sensor networks. In *Proceedings of IEEE MASS'04*.
8. J. Liu, J. Liu, J. Reich, P. Cheung, and F. Zhao. Distributed group management for track initiation and maintenance in target localization applications. In *Proceedings of IPSN'03*.
9. A. Mainwaring, R. Szewczyk, D. Culler, and J. Anderson. Wireless sensor networks for habitat monitoring. In *ACM International Workshop on Wireless Sensor Networks and Applications'02*.
10. S. Patten, S. Poduri, and B. Krishnamachari. Energy-quality tradeoffs for target tracking in wireless sensor networks. In *Proceedings of IPSN'03*.
11. Q. Wang, W. Chen, R. Zheng, K. Lee, and L. Sha. Acoustic target tracking using tiny wireless sensor devices. In *Proceedings of IPSN'03*.
12. X. Wang, G. Xing, Y. Zhang, C. Lu, R. Pless, and C. Gill. Integrated coverage and connectivity configuration in wireless sensor networks. In *Proceedings of ACM SenSys'03*.

13. T. Yan, T. He, and J. Stankovic. Differentiated surveillance for sensor networks. In *Proceedings of ACM SenSys'03*.
14. F. Ye, G. Zhong, J. Cheng, S. Lu, and L. Zhang. Peas: a robust energy conserving protocol for long-lived sensor networks. In *Proceedings of IEEE ICDCS'03*.
15. F. Zhao, J. Shin, and J. Reich. Information-driven dynamic sensor collaboration for tracking applications. In *IEEE Signal Processing Magazine*, March 2002.